JOURNAL OF AGRICULTURAL AND FOOD CHEMISTRY

Biologically Active Secondary Metabolites from *Ginkgo biloba*

ERDAL BEDIR,[†] IREM I. TATLI,[†] RIAZ A. KHAN,[†] JIANPING ZHAO,[†] SATOSHI TAKAMATSU,[†] LARRY A. WALKER,[†,‡] PETER GOLDMAN,[||,⊥] AND IKHLAS A. KHAN*[,†,§]

National Center for Natural Products Research, Research Institute of Pharmaceutical Sciences, and Department of Pharmacology and Pharmacognosy, School of Pharmacy, The University of Mississippi, University, Mississippi 38677; Beth Israel Deaconess Medical Center, Boston, Massachusetts 02215; and Harvard Medical School, Boston, Massachusetts 02115

Three new compounds, (7*E*)-2β,3α-dihydroxy-megastigm-7-en-9-one (**1**), 3-[5,7-dihydroxy-2-(4-methoxyphenyl)-4-oxo-4*H*-chromen-8-yl]-4-methoxybenzoic acid (**2**), and 4′-*O*-methyl myricetin 3-*O*-(6-*O*-α-L-rhamnopyranosyl)-β-D-glucopyranoside (**3**), were isolated from *Ginkgo biloba*, together with 27 known compounds. The structures of the new compounds were determined primarily from 1D- and 2D-NMR analysis. The 4-*O*-methylbenzoic acid structural feature at C-8 in **2** is encountered for the first time. The antioxidant activities of 29 compounds isolated from *Ginkgo biloba* were evaluated on intracellular reactive oxygen species in HL-60 cells. It was found that quercetin, kampferol, and tamarixetin had antioxidant activity that was approximately 3-fold greater than that of their respective glycosides and also approximately 3-fold greater than that of a standard ascorbic acid with an IC_{50} at maximum effectiveness.

KEYWORDS: ***Ginkgo biloba*; flavonoid; megastigmane; antioxidant activity**

INTRODUCTION

Ginkgo biloba (Ginkgoaceae) is the only representative of the ginkgophyta now in existence. It is a dioecious tree, with height up to 30 m and up to 9 m in circumference, which has been naturalized in Europe and America, although considered to be indigenous to China (*1*). *Ginkgo*, among the oldest surviving species of trees, flourished around 150 million years ago, but almost became extinct later during the ice age. The surviving wild stands were in China and parts of Asia. *Ginkgo* is among the most valued medicinal plants and has been since it was described in medical treatises of the ancient world; its fruit has been used for thousands of years by mankind (*2*). Prolific chemical and pharmacological studies have enhanced its traditional reputation and has made *Ginkgo* one of the most widely used phytopharmaceuticals in the world.

The unique botany of *Ginkgo* is rivaled by its chemistry. Its flavonoid content is particularly varied. The structural variations in the *Ginkgo* are represented by a variety of flavonol glycosides mainly based on kaempferol and quercetin as the aglycon with up to 3 sugar moieties. The minor components are derived from isorhamnetin, myricetin, 3′-methylmyricetin, apigenin, and luteolin as aglycons. The glycosides found are either monosaccharides containing β-D-glucose and α-L-rhamnose or disaccharides containing biloside and rutinose as sugars. Less common compounds from *Ginkgo* include flavonol glycosides esterified with *p*-coumaric acid (*3*). Besides their structural novelty, these compounds are useful in quality control of *Ginkgo* preparations. The bioactivity of *Ginkgo* preparations is attributed to the presence of a number of terpenoids (ginkgolides and bilobalide) and flavonoid constituents. The antioxidant, anti-ischemic, cardioprotective, neurosensory, cerebral, and anti-aging activity has been established on standardized *Ginkgo* extract, Egb 761 (*4*, *5*). However, the biological evaluation of *Ginkgo* flavonoids, and especially flavonol glycosides, has not been pursued because of the unavailability of individual flavonol glycosides. Therefore, the ongoing work of our group is focused on the isolation of these flavonol glycosides and evaluation of their antioxidant activities on intracellular reactive oxygen species (ROS) in HL-60 cells.

MATERIALS AND METHODS

General Experimental. IR spectra were recorded with an ATI Mattson Genesis Series FTIR spectrophotometer. The 1D- and 2D-NMR spectra were obtained on a Bruker Avance DRX 500 FT spectrometer operating at 500 and 125 MHz, respectively, for ^{1}H and ^{13}C measurements. The chemical shift values are reported as parts per million (ppm) units relative to tetramethylsilane (TMS) for ^{1}H- and ^{13}C-; and the coupling constants are in Hz (in parentheses). For the ^{13}C NMR spectra, multiplicities were determined by a DEPT experiment. High-resolution electrospray ionization Fourier transformation mass spectrometry (HRESIFTMS) were obtained using a Bruker BioApex FT-MS in ESI mode.

* Corresponding author. Phone: (662) 915-7821. E-mail: rikhan@olemiss.edu.
[†] National Center for Natural Products Research.
[‡] Department of Pharmacology.
[||] Beth Israel Deaconess Medical Center.
[⊥] Harvard Medical School.
[§] Department of Pharmacognosy.

10.1021/jf011682s CCC: $22.00
Published on Web 04/20/2002

Chromatographic Conditions. The following conditions were used: TLC, precoated Si 250F plates (Merck); developing system, EtOAc/MeOH/H_2O (100:17:13); visualization, vanillin/H_2SO_4; column chromatography, silica gel 230−400 mesh (Baker).

Extraction and Isolation. The dried and powdered leaves extract (0.9 kg) of *Ginkgo biloba*, provided by USA NutraSource, Inc., was extracted with acetone (20 L) at room temperature. The solvent was removed by rotary evaporation, yielding a 722.6 g extract. This acetone extract was subjected to vacuum liquid chromatography (VLC) using silica gel (1.25 kg) as the stationary phase eluting with hexane, diethyl ether, ethyl acetate, and acetone to give 13 fractions: fractions A−M. Fraction D (1.2 g) was subjected to vacuum liquid chromatography using reversed-phase material (Sepralyte 40 μm, 100 g), and eluted with H_2O/MeOH (100%−0%) to yield 5 fractions (fractions D1−D5). Fraction D4 (232.7 mg) was separated by silica gel column chromatography (120 g) using $CHCl_3$ and $CHCl_3$/MeOH (95:5) solvent systems to give 7 fractions (fractions D4a−D4g). Fraction D4a (27.4 mg) was purified on preparative RPTLC (50% MeOH in H_2O) to give **1** (3 mg, 0.004%). Fractions F, G, H, and I were combined and subjected to Sephadex LH-20 column chromatography (275 g) using MeOH to afford 3 fractions (FI-I, FI-II, FI-III). Fraction FI-II was chromatographed on RP material (Sepralyte 40 μm, 500 g), employing MeOH/H_2O (0%−100%) to give 7 fractions (FI-IIa−FI-IIg). Fraction FI−IIg (850 mg) was subjected to silica gel column chromatography (170 g) using $CHCl_3$/MeOH (97.5:2.5) and $CHCl_3$/MeOH (95:5) to yield 13 fractions (FI-IIg1−FI-IIg13). Fraction FI-IIg6 (9.4 mg) was purified further on a Sephadex LH-20 column (20 g) using MeOH to give **2** (6.8 mg, 0.009%). Fraction L (97.0 g) was applied to a Sephadex LH-20 column (275 g), and eluted with MeOH to give 4 fractions (L1−L4). Fraction L2 (90.0 g) was chromatographed on a polyamide column (400 g) using $CHCl_3$/MeOH/methyl ethyl ketone/acetone (3:2:0.5:0.5) to afford 5 fractions (L2a−L2d). Fraction L2d (75.0 g) was subjected to silica gel column chromatography (1.6 kg) using EtOAc/MeOH/H_2O mixtures (100:10:2.5, 100:10:5, and 100:15:10) and yielded 8 fractions (L2d1−L2d8). Fraction L2d7 (4.2 g) was subjected to Sephadex LH-20 column chromatography, and eluted with MeOH to give 4 fractions (L2d1A−L2d1D). Fraction L2d1B (1.2 g) was chromatographed on RP material (Sepralyte 40 μm), employing MeOH/H_2O (20%:40%) to give 4 fractions (L2d1B1−L2d1B2). Fraction L2d1B1 (156.0 mg) was further purified by Sephadex LH-20 column using MeOH to afford **3** (38.5 mg, 0.05%). Further studies performed on same material have resulted in the isolation of compounds **4**−**30**.

(7*E*)-2β,3α-Dihydroxy-megastigm-7-en-9-one (**1**). White powder. ^{1}H NMR (d_6-DMSO, 500 MHz) δ 6.59 (dd, J = 15.8, 9.8 Hz, H-7), 5.98 (d, J = 15.8 Hz, H-8), 3.42 (m, H-3), 2.78 (d, J = 9.3 Hz, H-2), 2.24 (s, H_3-10), 1.80 (m, H-4a), 1.48 (m, H-5), 1.38 (m, H-6), 0.87 (m, H-4b), 0.84 (s, H_3-11), 0.79 (s, H_3-12), 0.74 (d, J = 6.2 Hz, H_3-13). ^{13}C NMR ($CDCl_3$, 125 MHz) δ 198.7 (s, C-9), 148.3 (d, C-7), 134.1 (d, C-8), 82.4 (d, C-2), 70.5 (d, C-3), 57.7 (d, C-6), 41.4 (t, C-4), 39.7 (s, C-1), 30.3 (d, C-5), 27.3 (q, C-10), 21.1 (q, C-13), 17.2 (q, C-11), 15.3 (q, C-12). HRESIFTMS m/z [M + H]$^+$ calcd. for $C_{13}H_{22}O_3$, 227.3244; found, 227.3120.

3-[5,7-Dihydroxy-2-(4-methoxy-phenyl)-4-oxo-4*H*-chromen-8-yl]-4-methoxy-benzoic acid (**2**). Brown powder. $[\alpha]_D^{25}$ +10°(c 0.04, MeOH). UV (MeOH) λ_{max} (log ϵ) 216 (1.93), 272 (1.41), 324 (1.00) nm. IR (KBr) ν_{max} 3399, 2929, 1658, 1604, 1511, 1425, 1371, 1263, 1180, 1110, 1025, 835 cm^{-1}. ^{1}H NMR (d_6-DMSO, 500 MHz) δ 8.13 (dd, J = 8.6, 2.1 Hz, H-6″), and 7.98 (d, J = 2.1 Hz, H-2″), 7.54 (x2) (d, J = 8.8 Hz, H-2′ and H-6′), 7.17 (d, J = 8.7 Hz H-5″), 6.92 (×2) (d, J = 8.7 Hz, H-3′ and H-5′), 3.83 and 378 (each s, OCH_3). ^{13}C NMR (d_6-DMSO, 125 MHz) δ 184.7 (s, C-4), 176.0 (s, *C*OOH), 165.9 (s, C-2), 164.7 (s, C-4′), 163.9 (s, C-7), 162.5 (s, C-5), 161.8 (s, C-4″), 156.8 (s, C-9), 135.9 (d, C-2″), 132.8 (d, C-6″), 131.0 (s, C-1″), 129.5 (x2) (d, C-2′ and C-6′), 124.8 (s, C-1′), 121.9 (s, C-3″), 115.9 (x2) (d, C-3′ and C-5′), 111.6 (d, C-5″), 106.9 (d, C-8), 105.7 (s, C-10), 104.0 (d, C-3), 100.4 (d, C-6), 56.7 and 56.5 (each q, OCH_3). HRESIFTMS, m/z [M + Na]$^+$ calcd. for $C_{24}H_{18}O_8$, 457.3924; found, 457.1041; and LCMS m/z 433.0 [M − H]$^-$ (negative mode), and 435.0 [M + H]$^+$.

4′-*O*-Methylmyricetin 3-*O*-(6-*O*-α-L-rhamnopyranosyl)-β-D-glucopyranoside (**3**). Yellow powder. $[\alpha]_D^{25}$ −25°(c 0.04, MeOH). UV (MeOH) λ_{max} (log ϵ) 212 (1.94), 266 (0.96), 348 (0.74) nm. IR (KBr) ν_{max} 3351, 2929, 2360, 2341, 1726, 1654, 1602, 1504, 1452, 1365, 1301, 1203, 1060, 809 cm^{-1}. ^{1}H NMR (CD_3OD, 500 MHz) δ 7.26 (×2) (s, H-2′ and H-6′), 6.37 (br s, H-8), 6.20 (br s, H-6), 5.17 (d, J = 7.1 Hz, H-1$_{glu}$), 4.57 (br s, H-1$_{rha}$), 3.85* (H-6a$_{glu}$), 3.69* (br s H-2$_{rha}$), 3.57* (H-3$_{rha}$), 3.52* (H-2$_{glu}$), 3.50* (H-3$_{glu}$), 3.44* (H-5$_{rha}$), 3.42* (H-6b$_{glu}$), 3.39* (H-5$_{glu}$), 3.34* (H-4$_{glu}$), 3.33* (H-4$_{rha}$), 1.14 (d, J = 6.6 Hz, H_3-6$_{rha}$)(* signal pattern was unclear due to overlapping and assignments confirmed by G-DQFCOSY and G-HMQC). ^{13}C NMR ($CDCl_3$, 125 MHz) δ 178.4 (s, C-4), 165.4 (s, C-7), 161.8 (s, C-5), 157.6 (s, C-2), 157.5 (s, C-9), 150.2 (×2) (each s, C-3′ and C-5′), 138.5 (s, C-4′), 135.2 (s, C-3), 126.1 (s, C-1′), 109.6 (×2) (each d, C-2′ and C-6′), 104.7 (s, C-10), 103.4 (d, C-1$_{glu}$), 101.4 (d, C-1$_{rha}$), 99.2 (d, C-6), 94.1 (d, C-8), 77.1 (d, C-3$_{glu}$), 76.2 (d, C-5$_{glu}$), 74.7 (d, C-2$_{glu}$), 73.0 (d, C-4$_{rha}$), 71.3 (d, C-3$_{rha}$), 71.1 (d, C-2$_{rha}$), 70.5 (d, C-4$_{glu}$), 68.7 (d, C-5$_{rha}$), 67.6 (t, C-6$_{glu}$), 60.0 (q, OCH_3), 16.9 (q, C-6$_{rha}$). HRESIFTMS, m/z [M + Na]$^+$ calcd. for $C_{28}H_{32}O_{17}$, 640.4010; found, 640.5435.

Microplate Assay for the Detection of Oxidative Products. This method is based on a fluorimetric assay described by Rosenkranz et al. (*6*). Myelomonocytic HL-60 cells (1×10^6 cells/mL, ATCC) were suspended in RPMI 1640 medium with 10% FBS and antibiotics at 37 °C in 5% CO_2:95% air. A 125-μL aliquot of the cell suspension was added to a well on a 96-well plate. Different concentrations of the test materials were added, and the incubation continued for 30 min at which time the cells were stimulated by the addition of 100 ng/mL phorbol 12-myristate 13-acetate (Sigma). The incubation continued for another 30 min before adding 5 μg/mL 2′,7′-dichlorofluorescin diacetate (Molecular Probes), and the incubation continued for a further 15 min (the time needed for the nonfluorescent probe to diffuse into cells and the acetate groups to be hydrolyzed by cytoplasmic esterases to release 2′,7′-dichlorofluorescin, which is transformed by reactive oxygen species to the fluorescent dye 2′,7′-dichlorofluorescein). The ability of the test materials to inhibit exogenous cytoplasmic ROS-catalyzed oxidation of 2′,7′-dichlorofluorescin diacetate in HL-60 cells was measured by treated control incubations with and without the test materials. 2′,7′-Dichlorofluorescin formation, which reflects the effect of ROS and how it might be removed by various *Ginkgo* constituents, was measured using a CytoFluor 2350 fluorescence measurement system (Millipore) with excitation wavelength at 485 nm (bandwidth 20 nm) and emission at 530 nm (bandwidth 25 nm) (*6*). Ascorbic acid (Sigma), at maximally effective concentrations, served as a positive control.

RESULTS AND DISCUSSION

Structures of compounds **1**−**3** are shown in **Figure 1**. The molecular formula of **1** was determined as $C_{13}H_{22}O_3$ by HRESIMS, which exhibited a molecular ion at m/z 227.3120 [M + H]$^+$. Inspection of the ^{1}H NMR of **1** showed two tertiary methyl groups (δ 0.79 and 0.84, each s), a secondary methyl (δ 0.74, d, J = 6.2 Hz), as well as an acyl methyl (δ 2.24, s). Additionally, a trans disubstituted double bond (δ 5.98, d, J = 15.8 Hz, and δ 6.59, dd, J = 15.8, 9.8 Hz), and two oxymethine protons (δ 3.42, m and δ 2.78, d, J = 9.3 Hz) were observed. In the ^{13}C NMR spectrum of **1**, the resonances for the olefinic carbons and oxygenated carbons [δ 134.1 (d), 148.3 (d), and 82.4 (d), 70.5 (d), respectively] also supported the presence of the vinylic system and two oxymethine protons. Moreover, the resonance at δ 198.7 indicated one carbonyl carbon. Of the 3 degrees of unsaturation indicated by the molecular formula of **1**, two were attributed to a disubstituted double bond and carbonyl group, indicating the molecule to be monocyclic.

The combined use of the G-DQFCOSY and G-HMQC spectra of **1** allowed the assignment of one major spin system: H-2→H-8 (**Figure 2**). The spin system starts with the oxymethine proton at δ 2.78 (d, J = 9.3 Hz, H-2) which showed cross-peaks with another oxymethine proton (δ 3.42, m, H-3) in the G-DQFCOSY spectrum. H-3 is coupled with methylene protons of C-4 (1.80, m; 0.87, m, H_2-4) which displayed correlations with a methine proton at δ 1.48 (m, H-5), while the latter proton

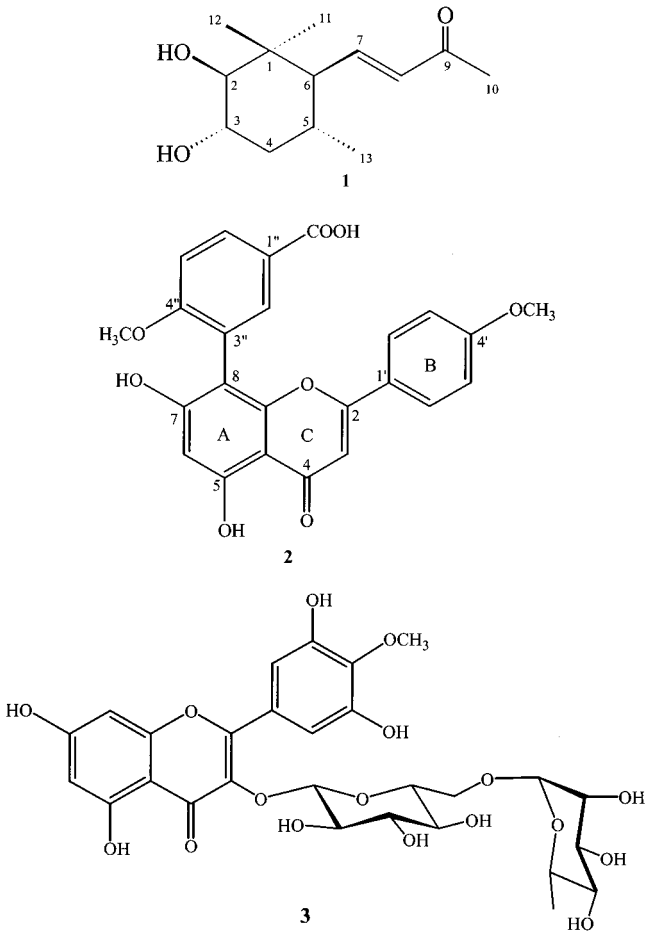

Figure 1. Structures of compounds **1**–**3**.

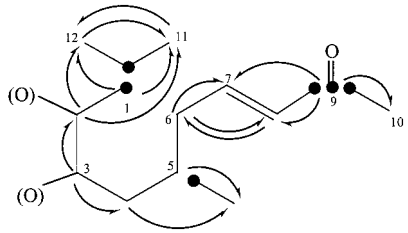

Figure 2. Partial structures deduced from DQFCOSY, HMQC, and key HMBC of **1**.

showed cross-peaks with H-6 (δ 1.38, m) and H_3-13 (δ 0.74, d, $J = 6.2$ Hz). H-6 coupled with an olefinic proton (6.59, dd, $J = 15.8$, 9.8 Hz, H-7) which, in turn, exhibited cross-peaks with the other olefinic proton (δ 5.98, d, $J = 15.8$ Hz, H-8). To associate the remaining fragments (two tertiary methyl groups and an acyl group) with the aforementioned spin system, it was necessary to perform a gradient long-range $^1H-^{13}C$ (G-HMBC) NMR measurement. The observation of the long-range correlations shown (**Figure 2**) revealed the molecule to be a megastigmane derivative (*7*, *8*).

The relative stereochemistry of **1** was resolved by NOESY data. The cross-peaks observed in the NOESY spectrum for H-2 to H_3-11 and H-6, and for H-6 to H_3-13 implied that these protons were cofacial (α), whereas observation of the key NOESY couplings from H-3 to H-5 and H_3-12 revealed that these protons occupy the β-face of the molecule. On the basis of all this evidence, the structure of **1** was established as (7*E*)-2β,3α-dihydroxy-megastigm-7-en-9-one.

Compound **2** was isolated as a yellow amorphous powder. Its ^1H- and ^{13}C NMR spectra showed the presence of aromatic

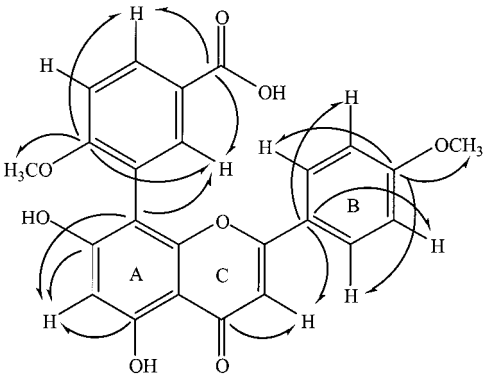

Figure 3. Key HMBC of **2**.

systems. The molecular formula of **2** was determined as $C_{24}H_{18}O_8$ by HRESIMS, which exhibited a molecular ion at *m/z* 457.1041 $[M + Na]^+$, and by LC−MS which provided ions at *m/z* 433.0 $[M - H]^-$ (negative mode), and 435.0 $[M + H]^+$ (positive mode).

Initial ^1H NMR and G-DQFCOSY studies of **2** defined an aromatic system at δ 8.13 (1H, dd, $J = 2.1$, 8.6 Hz, H-6″), 7.98 (1H, d, $J = 2.1$ Hz, H-2″), and 7.17 (1H, d, $J = 8.6$ Hz, H-5″). Taking into account the coupling pattern, i.e., one *meta* and one *ortho* coupling, it was inferred that **2** possesses a trisubstituted-aromatic ring. The chemical shifts of the *meta*-coupled protons observed at δ 8.13 and 7.98 indicated that these protons were adjacent to an electron-withdrawing substituent. This assumption was supported by long-range correlations in the G-HMBC spectrum between these protons and a carbonyl carbon at δ 176.0 (C-1″), suggesting the presence of a 3″,4″-disubstituted benzoyl moiety. Complete carbon assignment and the substitution pattern of this aromatic ring were achieved by inspection of the G-HMQC and G-HMBC spectra of **2**. The carbon signal at δ 161.8 indicating an electron-donating group, either a hydroxyl or a methoxyl group, showed HMBC connectivities to H-6″ (δ 8.13) and H-2″ (δ 7.98) (**Figure 3**), allowing it to be assigned unambiguously to C-4″ of the benzoyl moiety. Additionally, based on the HMBC correlations between C-4″ and the methoxy methyl at δ 3.78, the first methoxyl group was affixed to C-4″. As we did not observe any signal that indicated either acetylation or esterification, or an aldehyde proton signal, we presumed that the aromatic ring was a 3″,4″-disubstituted benzoic acid moiety. Therefore, C-3″ was assigned as the position for the linkage between the 3,4-disubstituted benzoic acid moiety and the remainder part of the molecule.

After subtraction of the 8 carbon resonances of the aforementioned aromatic system, the remaining 16 signals were attributable to a flavonoid skeleton (15 resonances) and a methoxy carbon. Of the remaining 6 protons, 4 were observed as coupled doublets (A_2B_2 system) at δ 6.92 (2H) and 7.54 (2H, $J = 8.8$ Hz). This suggested that the B-ring was *para*-substituted, with a hydroxyl or methoxyl group. This observation was supported by the ^{13}C NMR spectral data of **2** which indicated that a methoxyl group was attached to C-4′ based on the HMBC connectivities between C-4′ (δ 164.7) and the methyl signal at δ 3.82. The combined use of G-DQFCOSY, G-HMQC, and G-HMBC spectra of **2**, allowed for the complete assignment of the flavonoid skeleton and its substitution pattern. Thus, one of the two singlets at δ 6.65 showed correlations with the carbonyl carbon at δ 184.7, which was attributed to C-4, and C-1′ of the B-ring (δ 124.8), indicating that there was no substitution on C-3 of the C-ring. The remaining proton signal at δ 6.38 indicated 5-,7-, and either 6- or 8- substitution pattern for A-ring.

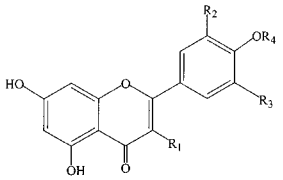

Compounds	R_1	R_2	R_3	R_4
Kaempferol (**4**)	OH	H	H	H
Quercetin (**5**)	OH	OH	H	H
Apigenin (**6**)	H	H	H	H
4′-*O*-Me apigenin (**7**)	H	H	H	CH_3
Myricetin (**8**)	OH	OH	OH	H
Tamarixetin (**9**)	OH	H	OH	CH_3

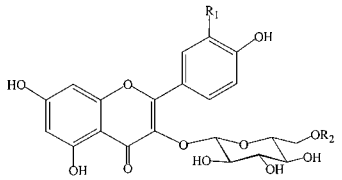

Compounds	R_1	R_2
10	H	H
11	H	α-L-rhamnosyl
12	OH	H
13	OH	α-L-rhamnosyl

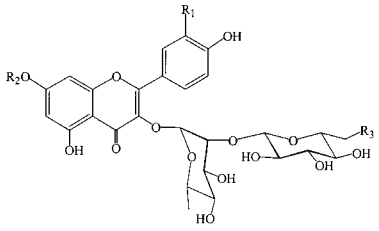

Compounds	R_1	R_2	R_3
14	H	H	H
15	H	H	*p*-coumaroyl
16	OH	H	H
17	OH	H	*p*-coumaroyl
18	H	β-D-glucosyl	*p*-coumaroyl

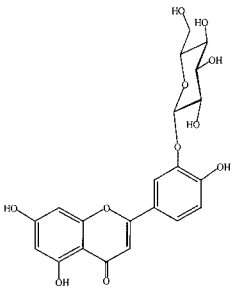

3′-*O*-(β-D-glucopyranosyl)Luteolin (**19**)

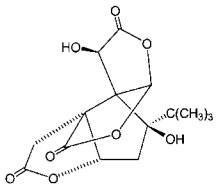

Bilobalide (**24**)

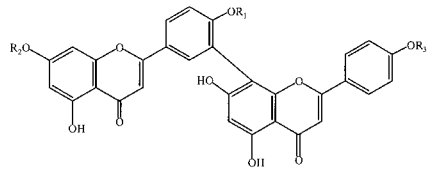

Compounds	R_1	R_2	R_3
Amentoflavone (**20**)	H	H	H
Bilobetin (**21**)	CH_3	H	H
Ginkgetin (**22**)	CH_3	CH_3	H
Sciadopitysin (**23**)	CH_3	CH_3	CH_3

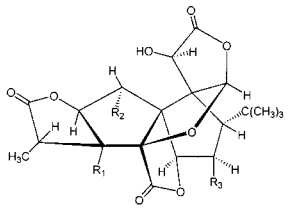

Compounds	R_1	R_2	R_3
Ginkgolide A (**25**)	OH	H	H
Ginkgolide B (**26**)	OH	OH	H
Ginkgolide C (**27**)	OH	OH	OH
Ginkgolide J (**28**)	OH	H	OH

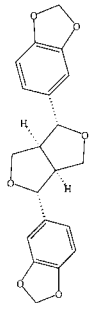

Sesamin (**29**)

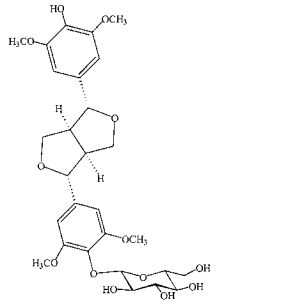

Syringaresinol-4′-*O*-β-D-glucopyranoside (**30**)

Figure 4. Structures of compounds **4**–**30**.

Therefore, the aglycon of **2** was characterized as an *O*-methyl derivative of apigenin with an A-ring substitution (*9*). The carbon resonances at δ 162.5 and 163.9 were attributed to C-5 and C-7, respectively, a characteristic feature of the 5,7-dihydroxy A-ring (*9*). On the basis of long-range connectivities in the HMBC spectrum between the aromatic proton signal at δ 6.38, and C-5 and C-7, the proton was readily assigned to H-6, implying the position of the linkage as C-8. The large deshielding of C-8 (ca. 10 ppm) and the HMBC connectivities between C-8 (δ 106.9) and H-2″ of the benzoic acid moiety (δ 7.98), and H-6 (δ 6.38) confirmed our assumptions. Consequently, the structure of **2** was established as 3-[5,7-dihydroxy-2-(4-methoxy-phenyl)-4-oxo-4*H*-chromen-8-yl]-4-methoxybenzoic acid. Compound **2** represents the first example of the series of flavonoids possessing a 4-*O*-methyl-benzoic acid at C-8. The significance of this metabolite is not fully understood. However, because biflavonoids are produced in the plant by phenol oxidative coupling of appropriate flavonoid precursors (*10*, *11*), the resemblance of *Ginkgo biloba* biflavonoids and **2** suggests compound **2** to be a product of catabolism.

The HRESIMS of **3** provided an $[M + Na]^+$ ion at *m*/*z* 640.5435 indicating the molecular formula $C_{28}H_{32}O_{17}$. The IR spectrum of **3** showed a large hydroxyl absorbance (3351 cm^{-1}) and a carbonyl absorbance at ca. 1654 cm^{-1}.

The ^1H NMR spectrum of the aglycon moiety of **3** displayed the typical spin patterns of an *O*-methylated myricetin moiety (*12*): two *meta* coupled doublets at δ 6.20 and 6.37 for the A-ring correlated with carbons at δ 99.2 and 94.1 in the G-HMQC spectrum, and a two proton singlet at δ 7.26 for the 3′,4′,5′-trioxygenated B-ring. The three-proton *O*-methyl singlet at δ 3.91 showed long-range correlation with the carbon resonance at δ 138.5 in the G-HMBC spectrum, hence locating the methoxyl group to C-4′ of the ring. The resonances of two anomeric protons, observed in the low-field region at δ 5.17

Table 1. Antioxidant Effect of Compounds **2**–**30** in HL-60 Cells with 2′,7′-Dichlorofluorescin Diacetate

compound	IC_{50} (μg/mL)	inhibition (%) at 62.5 (μg/mL)
2	18.0	
3	12.0	
kaempferol (**4**)	1.2	
quercetin (**5**)	0.6	
apigenin (**6**)		28.5
4′-*O*-methyl apigenin (**7**)		0
myricetin (**8**)	3.9	
tamarixetin (**9**)	1.5	
10	4.4	
11	5.5	
12	2.9	
13	6.0	
14	33.0	
15	25.0	
16	2.4	
17	3.0	
18	6.9	
19	5.0	
amentoflavone (**20**)		10.6
bilobetin (**21**)		34.3
ginkgetin (**22**)		19.0
sciadopitysin (**23**)		37.3
bilobalide (**24**)		28.0[a]
ginkgolide A (**25**)		28.9[a]
ginkgolide B (**26**)		37.2[a]
ginkgolide C (**27**)		26.4[a]
ginkgolide J (**28**)		34
sesamin (**29**)		32.6
30	8.0	
ascorbic acid	2.6	

[a] Inhibition (%) at 31.3 μg/mL

(d, $J = 7.5$ Hz) and 4.57 (br. s), implied that compound **3** was a disaccharide of 4′-*O*-methylmyricetin.

The full assignment of the proton and carbon signals of the aglycon and sugar moieties of **3**, secured by G-DQFCOSY, G-HMQC, and G-HMBC spectra, and the comparison of these data with those of 3-*O*-[6-*O*-(α-L-rhamnopyranosyl)-β-D-glucopyranosyl] myricetin previously isolated from *Ginkgo biloba* (*13*), indicated that **3** was its 4′-*O*-methyl derivative, i.e., myricetin 4′-*O*-methyl 3-*O*-(6-*O*-α-L-rhamnopyranosyl)-β-D-glucopyranoside.

From the leaves of *Ginkgo biloba*, quercetin, kaempferol, myricetin, apigenin, 4′-*O*-methylapigenin, tamarixetin, amentoflavone, ginkgetin, bilobetin, sciadopitysin, sesamin, 3-*O*-(β-D-glucopyranosyl) quercetin, 3-*O*-(β-D-glucopyranosyl) kaempferol, 3-*O*-[2-*O*-(6-*O*-{*p*-hydroxy-*trans*-cinnamoyl}-β-D-glucopyranosyl)-α-L-rhamnopyranosyl] quercetin, 3-*O*-[2-*O*-(β-D-glucopyranosyl)-α-L-rhamnopyranosyl] kaempferol, 3-*O*-[2-*O*-(6-*O*-{*p*-hydroxy-*trans*-cinnamoyl}-β-D-glucopyranosyl)-α-L-rhamnopyranosyl] kaempferol, 3-*O*-[2-*O*-(β-D-glucopyranosyl)-α-L-rhamnopyranosyl] quercetin, 3-*O*-[2-*O*-(6-*O*-{*p*-hydroxy-*trans*-cinnamoyl}-β-D-glucopyranosyl)-α-L-rhamnopyranosyl] quercetin, 3-*O*-[6-*O*-(α-L-rhamnopyranosyl)-β-D-glucopyranosyl] quercetin, 3-*O*-[6-*O*-(α-L-rhamnopyranosyl)-β-D-glucopyranosyl] kaempferol, 3′-*O*-(β-D-glucopyranosyl) luteolin, 3-*O*-[6-*O*-(α-L-rhamnopyranosyl)-β-D-glucopyranosyl]-3′-*O*-methylmyricetin, syringaresinol-4′-*O*-β-D-glucopyranoside, ginkgolides A, B, C, J, and bilobalide were also isolated and identified by comparison of their ^{1}H- and ^{13}C NMR spectral data with literature values (*14*−*23*). This appears to be the first report of the occurrence of 4′-*O*-methylapigenin, and syringaresinol-4′-*O*-β-D-glucopyranoside in *Ginkgo biloba*.

Earlier studies of plant-derived antioxidants have examined the reduction potential or radical-scavenging effects of natural products in solution-based chemical assays (*24*−*26*). Fluorescence technology has made it possible to evaluate antioxidants in live cells using specific probes such as 2′,7′dichlorofluorescin diacetate. This assay is based on the detection of intracellular respiratory burst activity in phagocytic cells such as neutrophils and macrophages (*6*). We evaluated the antioxidant activity of compounds **2**-**30** (structures of **4**−**30** are shown in **Figure 4**), isolated from *Ginkgo biloba*, which we compared with the known antioxidant ascorbic acid using the assay. Ginkgolides (**25**−**28**) and bilobalide (**24**), which are unique constituents of *Ginkgo biloba*, were not very potent inhibitors of the respiratory burst; their inhibitions range between 28% and 37.3% at 31.3 μg/mL. Strong antioxidant activity, as expected, was observed for the flavonoids, although not for the biflavonoids (**20**−**24**) (**Table 1**). Among the aglycons, a hydroxyl group in the C ring (3-OH), e. g., kaempferol (**4**), quercetin (**5**), myricetin (**8**), and tamarixetin (**9**), conferred more antioxidant activity than if this group is lacking, e. g., apigenin (**6**) 4′-*O*-methylapigenin (**7**) and biflavonoids (**20**−**24**). The importance of a hydroxyl group at either C-3′ or C-4′ of the B ring for high antioxidant capacity of flavonoids has been described (*27*−*29*) and is confirmed by our findings, which also suggest the importance of *ortho*-hydroxyl groups at C-3′ and C-4′ as in quercetin (**5**), which is the most potent antioxidant of the compounds tested. Thus, quercetin (**5**) (IC_{50}, 0.6 μg/mL), with nearly 4 times the potency of ascorbic acid (IC_{50}, 2.6 μg/mL), is more potent than tamarixetin (**9**) (IC_{50}, 1.5 μg/mL) in which the 4′-hydroxy group is methylated, and myricetin (**8**) (IC_{50}, 3.9 μg/mL) which bears the 3,4,5-trihydroxy B ring. Moreover, our finding that kaempferol (**4**) (IC_{50}, 1.2 μg/mL) is more potent than **9** contradicts a conclusion of Cao et al. (*28*) that antioxidant potency increases with the number of hydroxyl groups. **Table 1** also demonstrates that glycosylation of flavonoids diminishes their antioxidant effect. Thus, the IC_{50} values of glycosides **10**−**13** indicate that they have only approximately one-quarter the potency of their respective aglycons (**4** and **5**), a phenomenon that did not appear to be influenced by any variation of the sugar moiety.

The order of antioxidant potency of glycosides in the assay was as follows: quercetin-3-glucorhamnoside (**16**) > quercetin-3-glucoside (**12**) > kaempferol-3-glucoside (**10**) > luteolin-3′-glucoside (**19**) > kaempferol-3-rhamnoglucoside (**11**) > quercetin-3-rhamnoglucoside (**13**) > kaempferol-3-glucorhamnoside (**14**). The acylation of glycosides (**14** and **16**) by *p*-coumaric acid, distinctive compounds for *Ginkgo biloba* (**15**, **17**, and **18**; IC_{50} values 25.0, 3.0, and 6.9 μg/mL, respectively) led to minor changes or was devoid of any effect. The results suggest that the co-occurrence of hydroxyl group at C-3 (ring C), and *ortho*-hydroxyl groups at C-3′ and C-4′ (ring B) is essential for this class of compounds to exhibit strong antioxidant activity.

ACKNOWLEDGMENT

We are grateful to Dr. Chuck Dunbar for conducting the HRESIFTMS analysis. We also thank Mr. Frank Wiggers for his assistance in obtaining the 2D-NMR spectra.

LITERATURE CITED

(1) Kramer, K. U.; Green, P. S. *The Families and Genera of Vascular Plants - Pteridophytes and Gymnosperms*; Springer-Verlag: Berlin, 1990; pp 284−289.

(2) Hobbs, C.; *Ginkgo: Elixir of Youth*; Botanica Press: Capitola, CA, 1991.

(3) Sticher, O.; Meier, B.; Hasler, A. The Analysis of *Ginkgo* flavonoids. In *Ginkgo biloba*; van Beek, T. A., Ed.; Harwood Academic Publishers: Amsterdam, The Netherlands, 2000; pp 179−202.

(4) DeFeudis, F. V.; Drieu, K. *In vitro* studies of the pharmacological and biochemical activities of *Ginkgo biloba* extract (EGb 761) and its constituents. In *Ginkgo biloba*; van Beek, T. A., Ed.; Harwood Academic Publishers: Amsterdam, The Netherlands, 2000; pp 279−302.

(5) Drieu, K.; DeFeudis, F. V. *In vivo* studies of the pharmacological and biochemical activities of *Ginkgo biloba* extract (EGb 761) and its constituents. In *Ginkgo biloba*; van Beek, T. A., Ed.; Harwood Academic Publishers: Amsterdam, The Netherlands, 2000; pp 303−330.

(6) Rosenkranz, A. R.; Schmaldienst, S.; Stuhlmeier, K. M.; Chen, W. J.; Knapp, W.; Zlabinger, G. J. A microplate assay for the detection of oxidative products using 2′,7′-dichlorofluorescin-diacetate. *J. Immunol. Methods* **1992**, *156*, 39−45.

(7) Chakravarty, A. K.; Das, B.; Masuda, K.; Ageta, H. Glycoric acid possessing a new 10-normegastigmane skeleton from *Glycosmis arborea*. *Chem. Pharm. Bull.* **1996**, *44*, 1421−1423.

(8) Otsuka, H.; Kido, M.; Tsukihara, T.; Tsukihara, K.; Takeda, Y.; Yamasaki, K.; Takeda, Y. Absolute Structure of Ionol Glucoside: A single-crystal X-ray analysis of dendranthemoside A pentaacetate. *Chem. Pharm. Bull.* **1993**, *41*, 1860−1862.

(9) Khallouki, F.; Hmamouchi, M.; Younos, C.; Soulimani, R.; Essassi, E. M. A new flavonoid from the aerial parts of *Chrysanthemum viscidehirtum*. *Fitoterapia* **2000**, *71*, 413−416.

(10) Kandaswami, C.; Vaidyanathan, C. S. Oxidation of catechol in plants. II. Enzymic conversion of catechol to diphenylenedioxide 2,3-quinone in the leaves of *Tecoma stans* L. *Indian J. Biochem. Biophys.* **1973**, *10*, 23−26.

(11) Hakamatsuka, T.; Shinkai, K.; Noguchi, H.; Ebizuka, Y.; Sankawa, U. Isoflavone dimers from yeast extract-treated cell suspension cultures of *Pueraria lobata*. *Z. Naturforsch., C: J. Biosci.* **1992**, *47*, 177−182.

(12) Iyengar, M. A.; Bhat, U. G.; Katti, S. B.; Wagner, H.; Seligmann, O.; Herz, W. Mearnsetin. A rare flavonol from *Liatris pauciflora.* *Indian J. Chem., Sect. B* **1976**, *14B*, 714.

(13) Hasler, A. R. Flavonoide aus *Ginkgo biloba* L. und HPLC-Analytik von Flavonoiden in verschiedenen Arzneipflanzen. Ph.D. Thesis, ETH (Nr. 9353), Zurich, Switzerland, 1990.

(14) Vanhaelen, M.; Vanhaelen-Fastre, R. Flavonol triglycosides from *Ginkgo biloba*. *Planta Med*. **1989**, *55*, 202.

(15) Lobstein-Guth, A.; Briancon-Scheid, F.; Victoire, C.; Haag-Berruier, M.; Anton, R. Isolation of amentoflavone from *Ginkgo biloba. Planta Med.* **1988**, *54*, 555−556.

(16) Victoire, C.; Haag-Berruier, M.; Lobstein-Guth, A.; Balz, J. P.; Anton, R. Isolation of flavonol glycosides from *Ginkgo biloba* leaves. *Planta Med.* **1988**, *54*, 245−247.

(17) Nasr, C.; Lobstein-Guth, A.; Haag-Berruier, M.; Anton, R. Quercetin coumaroyl glucorhamnoside from *Ginkgo biloba*. *Phytochemistry* **1987**, *26*, 2869−2870.

(18) Nasr, C.; Lobstein-Guth, A.; Haag-Berruier, M.; Anton, R. Kaempferol coumaroyl glucorhamnoside from *Ginkgo biloba*. *Phytochemistry* **1986**, *25*, 770−771.

(19) Kang, S. S.; Kim, J. S.; Kwak, W. J.; Kim, K. H. Flavonoids from the leaves of *Ginkgo biloba. Saengyak Hakhoechi* **1990**, *21*, 111−120.

(20) Struck, R. F.; Kirk, M. C. Methylated flavonols in the genus *Gossypium*. *J. Agric. Food Chem.* **1970**, *18*, 548−549.

(21) Pelter, A.; Ward, R. S.; Rao, E. V.; Sastry, K. V. General methods for the assignment of stereochemistry to 2,6-diaryl-3,7-dioxa-bicyclo[3.3.0]octane lignans. *Tetrahedron* **1976**, *32*, 2783−2788.

(22) Lami, N.; Kadota, S.; Kikuchi, T.; Momose, Y. Constituents of the roots of *Boerhaavia diffusa* L. III. Identification of Ca^{2+} channel antagonistic compound from the methanol extract. *Chem. Pharm. Bull*. **1991**, *39*, 1551−1555.

(23) Roumestand, C.; Perly, B.; Hosford, D.; Braquet, P. Proton and Carbon-13 NMR of Ginkgolides. *Tetrahedron* **1989**, *45*, 1975−1983.

(24) Cavin, A.; Potterat, O.; Wolfender, J. L.; Hostettman, K.; Dyatmyko, W. Use of on-flow LC/^{1}H NMR for the study of an antioxidant fraction from *Orophea enneandra* and isolation of a polyacetylene, lignans, and a tocopherol derivative. *J. Nat. Prod*. **1998**, *61*, 1497−1501.

(25) Masuda, T.; Matsumura, H.; Oyama, Y.; Takeda, Y.; Jitoe, A.; Kida, A.; Hidaka, K. Synthesis of (±)-cassumunins A and B, new curcuminoid antioxidants having protective activity of the living cell against oxidative damage. *J. Nat. Prod*. **1998**, *61*, 609−613.

(26) Westenburg, H. E.; Lee, K. J.; Lee, S. K.; Fong, H. H. S.; van Breemen, R. B.; Pezzuto, J. M.; Kinghorn, A. D. Activity-guided isolation of antioxidative constituents of *Cotinus coggygria*. *J. Nat. Prod*. **2000**, *63*, 1696−1698.

(27) Bors, W.; Heller, W.; Michel, C.; Saran, M. Flavonoids as antioxidants: determination of radical-scavenging efficiencies. *Methods Enzymol*. **1990**, *186*, 343−355.

(28) Cao, G. H.; Sofic, E.; Prior, R. L. Antioxidant and prooxidant behaviour of flavonoids: Structure−activity relationships. *Free Radical Biol. Med.* **1997**, *22*, 749−760.

(29) Rice-Evans, C.; Miller, N. J.; Paganga, G. Structure−antioxidant activity relationships of flavonoids and phenolic acids. *Free Radical Biol. Med.* **1996**, *20*, 933−956.

Received for review December 20, 2001. Revised manuscript received March 12, 2002. Accepted March 15, 2002. This work was supported in part by the United States Department of Agriculture, ARS Specific Cooperative Research Agreement 58-6408-7-012 and by RO1 AT00607 from the National Center for Complementary and Alternative Medicine.

JF011682S